$$\begin{bmatrix} x_a \\ x_b \end{bmatrix} = \begin{bmatrix} u_1 \\ u_3 \end{bmatrix} + \frac{u_2}{\Delta t}\begin{bmatrix} ct_2^a(s_{11}t_{22} - s_{21}t_{12}) \\ \frac{c_2^a}{s_2^b}(s_{12}t_{22} - s_{22}t_{12}) \end{bmatrix} + \frac{u_4}{\Delta t}\begin{bmatrix} \frac{c_2^b}{s_2^a}(s_{21}t_{11} - s_{11}t_{21}) \\ ct_2^b(s_{22}t_{11} - s_{12}t_{21}) \end{bmatrix} \quad \text{(A-3a,b)}$$

$$\begin{bmatrix} y_a \\ y_b \end{bmatrix} = \begin{bmatrix} v_1 \\ v_3 \end{bmatrix} + \frac{v_2}{\Delta t}\begin{bmatrix} ct_2^a(s_{11}t_{22} - s_{21}t_{12}) \\ \frac{c_2^a}{s_2^b}(s_{12}t_{22} - s_{22}t_{12}) \end{bmatrix} + \frac{v_4}{\Delta t}\begin{bmatrix} \frac{c_2^b}{s_2^a}(s_{21}t_{11} - s_{11}t_{21}) \\ ct_2^b(s_{22}t_{11} - s_{12}t_{21}) \end{bmatrix} \quad \text{(A-3c,d)}$$

$$\begin{bmatrix} s_{11} \\ s_{12} \end{bmatrix} = \frac{\left(h_{11}\begin{pmatrix}\eta_a \\ \eta_b\end{pmatrix} + h_{12}\right)}{z_0\mu_d G}\begin{bmatrix}\gamma_a \\ \gamma_b\end{bmatrix}$$

$$\begin{bmatrix} s_{21} \\ s_{12} \end{bmatrix} = \frac{\left(h_{21}\begin{pmatrix}\eta_a \\ \eta_b\end{pmatrix} + h_{22}\right)}{z_0\mu_d G}\begin{bmatrix}\gamma_a \\ \gamma_b\end{bmatrix} \quad \text{(A-4a,b,c,d)}$$

$$\begin{bmatrix} t_{11} \\ t_{12} \end{bmatrix} = \left\{\frac{-\beta y_0}{(\alpha^2+\beta^2)\gamma_3}\left(\alpha\begin{bmatrix}\eta_a \\ \eta_b\end{bmatrix} + \beta\right) + \frac{\alpha\gamma_3}{(\alpha^2+\beta^2)z_0}\left(\beta\begin{bmatrix}\eta_a \\ \eta_b\end{bmatrix} - \alpha\right)\right\}ct_3 \quad \text{(A-5a,b)}$$

$$\begin{bmatrix} t_{21} \\ t_{22} \end{bmatrix} = \left\{\frac{\alpha y_0}{(\alpha^2+\beta^2)\gamma_3}\left(\alpha\begin{bmatrix}\eta_a \\ \eta_b\end{bmatrix} + \beta\right) + \frac{\beta\gamma_3}{(\alpha^2+\beta^2)z_0}\left(\beta\begin{bmatrix}\eta_a \\ \eta_b\end{bmatrix} - \alpha\right)\right\}ct_3 \quad \text{(A-5c,d)}$$

with

$$\begin{bmatrix} u_1 \\ u_2 \end{bmatrix} = \frac{\gamma_a(h_{11}\eta_a + h_{12})}{z_0\mu_d G}\begin{bmatrix} ct_2^a \\ th_2^a \end{bmatrix} - \frac{\beta ct_1 y_0(\alpha\eta_a + \beta)}{\gamma_1(\alpha^2+\beta^2)} + \frac{\alpha\gamma_1 ct_1(\beta\eta_a - \alpha)}{z_0(\alpha^2+\beta^2)} \quad \text{(A-6a,b)}$$

$$\begin{bmatrix} u_3 \\ u_4 \end{bmatrix} = \frac{\gamma_b(h_{11}\eta_b + h_{12})}{z_0\mu_d G}\begin{bmatrix} ct_2^b \\ th_2^b \end{bmatrix} - \frac{\beta ct_1 y_0(\alpha\eta_b + \beta)}{\gamma_1(\alpha^2+\beta^2)} + \frac{\alpha\gamma_1 ct_1(\beta\eta_b - \alpha)}{z_0(\alpha^2+\beta^2)} \quad \text{(A-6c,d)}$$

$$\begin{bmatrix} v_1 \\ v_2 \end{bmatrix} = \frac{\gamma_a(h_{21}\eta_a + h_{22})}{z_0\mu_d G}\begin{bmatrix} ct_2^a \\ th_2^a \end{bmatrix} + \frac{\alpha ct_1 y_0(\alpha\eta_a + \beta)}{\gamma_1(\alpha^2+\beta^2)} + \frac{\beta\gamma_1 ct_1(\beta\eta_a - \alpha)}{z_0(\alpha^2+\beta^2)} \quad \text{(A-7a,b)}$$

$$\begin{bmatrix} v_3 \\ v_2 \end{bmatrix} = \frac{\gamma_b(h_{21}\eta_b + h_{22})}{z_0\mu_d G}\begin{bmatrix} ct_2^b \\ th_2^b \end{bmatrix} + \frac{\alpha ct_1 y_0(\alpha\eta_b + \beta)}{\gamma_1(\alpha^2+\beta^2)} + \frac{\beta\gamma_1 ct_1(\beta\eta_b - \alpha)}{z_0(\alpha^2+\beta^2)}, \quad \text{(A-7c,d)}$$

where $z_0 = j\omega\mu_0$, $\mu_d = \mu_{xx}\mu_{zz} - \mu_{xz}\mu_{zx}$, and

$$G = \alpha^2\mu_{xx} + \beta^2\mu_{zz} + \alpha\beta(\mu_{xz} + \mu_{zx}) - k_0^2\varepsilon_{yy}\mu_d. \quad \text{(A-7e)}$$

Variables γ_1, $\gamma_{a,b}$, γ_3 are roots of characteristic equations in regions 1, 2, and 3, respectively. The remaining constants appearing in the above equations are given as

$$z_0 = j\omega\mu_0 \qquad y_0 = j\omega\varepsilon_0 \quad \text{(A-8a,b)}$$

$$s_2^{a,b} = \sinh\gamma_{a,b}d \qquad c_2^{a,b} = \cosh\gamma_{a,b}d \quad \text{(A-9a,b)}$$

$$ct_2^{a,b} = \coth\gamma_{a,b}d \qquad th_2^{a,b} = \tanh\gamma_{a,b}d \quad \text{(A-9c,d)}$$

$$ct_1 = \coth\gamma_1 h_2 \qquad ct_3 = \coth\gamma_3 h_1 \quad \text{(A-10a,b)}$$

where ω is the angular frequency.

References

[1] B. Bhat and S. K. Koul, *Analysis, Design and Application of Fin Lines.* Norwood, MA: Artech House, 1987.

[2] S. K. Koul and R. Khanna, "Broadside-coupled rectangular resonators in suspended stripline with single and double dielectrics," *IEE Proc.*, Pt. H, vol. 137, no. 6, pp. 411–414, Dec. 1990.

[3] T. Itoh, "Analysis of microstrip resonators," *IEEE Trans. Microwave Theory Tech.*, vol. MTT-22, no. 11, pp. 946–952, Nov. 1974.

[4] S. Mao, S. Jones, and G. D. Vendilin, "Millimeter-wave integrated circuits," *IEEE Trans. Microwave Theory Tech.*, vol. MTT-16, no. 7, pp. 455–461, July 1968.

[5] T. Uwano, "A small dielectric TEM mode resonator with crossing slot and its application to a cellular radio VCO," *IEEE Trans. Microwave Theory Tech.*, vol. MTT-22, no. 11, pp. 946–952, Nov. 1974.

[6] A. K. Agrawal and B. Bhat, "Characteristics of coupled rectangular slot resonators in fin-line configurations," *Int. J. Electron.*, vol. 58, no. 5, pp. 781–792, 1985.

[7] N. G. Alexopoulos, "Integrated structures on anisotropic substrates," *IEEE Trans. Microwave Theory Tech.*, vol. MTT-33, no. 10, pp. 847–881, Oct. 1985.

[8] A. Deutsch *et al.*, "Dielectric anisotropy of BPDA-PDA polymide and its effect on electrical characteristics of interconnects," in *Proc. 2nd Meet. Elect. Performance Electron., Packaging*, Oct. 1993, pp. 152–154.

[9] Y. Chen and B. Beker, "Spectral-domain analysis of open and shielded slotlines printed on various anisotropic substrates," *IEEE Trans. Microwave Theory Tech.*, vol. MTT-41, no. 11, pp. 1872–1877, Nov. 1993.

[10] Y. Chen and B. Beker, "Dispersion characteristics of open and shielded microstrip lines under a combined principal axes rotation of electrically and magnetically anisotropic substrates," *IEEE Trans. Microwave Theory Tech.*, vol. 41, no. 4, pp. 673–679, Apr. 1993.

[11] T. Itoh and W. Menzel, "A full-wave analysis method for open microstrip structures," *IEEE Trans. Antennas and Propagat.*, vol. AP-29, pp. 63–68, 1981.

Characterization of Cylindrical Microstriplines Mounted Inside a Ground Cylindrical Surface

Ruenn-Bo Tsai and Kin-Lu Wong

***Abstract*—A full-wave analysis for the frequency-dependent characteristics of a cylindrical microstripline mounted inside a ground cylindrical surface is presented. Numerical results of the effective dielectric constant and characteristic impedance for various microstripline parameters are calculated and analyzed. Strong dispersive behavior is observed for such cylindrical microstriplines.**

I. Introduction

For many practical applications, microstrip antennas need to be conformed to curved surfaces. This also makes necessary the design of conformal microstrip circuits that form the excitation network of the antenna. This paper presents the study of a microstripline printed on the inner surface of a cylindrical substrate that is enclosed by a conducting ground cylinder. This kind of cylindrical microstripline can find applications in feeding a slot-coupled cylindrical microstrip antenna [1]. In this case, the energy can be coupled from the microstripline to the antenna through a coupling slot in the cylindrical

Manuscript received August 16, 1994; revised December 19, 1994. This work was supported by the National Science Council of the Republic of China Grant NSC83-0404-E-110-017.

The authors are with the Department of Electrical Engineering, National Sun Yat-Sen University, Kaohsiung, Taiwan 804, R.O.C.

IEEE Log Number 9412031.

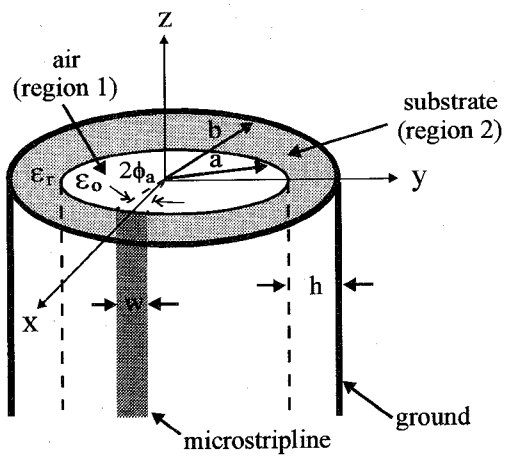

Fig. 1. Geometry of a cylindrical microstripline mounted inside a cylindrical ground surface.

ground plane. Such an accurate design of this new configuration of cylindrical microstriplines is still not available in the open literature, we present here a full-wave analysis of such a microstripline. The frequency-dependent characteristics of the effective dielectric constant and characteristic impedance of the microstripline are calculated and analyzed.

II. Theoretical Formulation

Fig. 1 shows the geometry under consideration. The microstripline is assumed to be infinitely long and with a width of $w = 2a\phi_a$, and the substrate has a thickness of $h\,(= b-a)$ and a relative permittivity of ϵ_r. Given a narrow microstripline (i.e., $w \ll 2\pi/k_e$, k_e is the effective wavenumber), the surface current density on the microstripline can be approximated by

$$\vec{J}(\phi, z) = \hat{z}\, J_z(\phi) e^{jk_e z} \tag{1}$$

with

$$J_z(\phi)\begin{cases} \frac{1}{a\pi\sqrt{\phi_a^2-\phi^2}}, & |\phi| \le \phi_a \\ 0, & |\phi| > \phi_a \end{cases}. \tag{2}$$

After expanding the spectral-domain Maxwell's equations in cylindrical coordinates, we find the $\hat{z}$-component electric field $\tilde{E}_z(\rho, n, k_z)$ and magnetic field $\tilde{H}_z(\rho, n, k_z)$ to satisfy the following wave equation:

in region 1 (the inner free-space region)

$$\left[\frac{1}{\rho}\frac{d}{d\rho}\left(\rho\frac{d}{d\rho}\right) + \left(k_0^2 - k_z^2\right)\right]\tilde{\Psi}_z(\rho, n, k_z) = 0 \tag{3}$$

and, in region 2 (the substrate region)

$$\left[\frac{1}{\rho}\frac{d}{d\rho}\left(\rho\frac{d}{d\rho}\right) + \left(\epsilon_r k_0^2 - k_z^2\right)\right]\tilde{\Psi}_z(\rho, n, k_z) = 0 \tag{4}$$

where $\tilde{\Psi}_z$ denotes $\tilde{E}_z$ or $\tilde{H}_z$; $k_0 = \omega\sqrt{\mu_0\epsilon_0}$. The field spectral amplitude is defined as

$$\tilde{\Psi}(\rho, n, k_z) = \frac{1}{2\pi}\int_{-\pi}^{\pi}\int_{-\infty}^{\infty}\Psi(\rho, \phi, z)e^{-jn\phi}e^{-jk_z z}\,dz\,d\phi. \tag{5}$$

The above spectral-domain wave equations can be solved using the Green's function technique. The longitudinal electric field at $\rho = a$ is related to the surface current density on the microstripline as (in the spectral domain) [2], [3]

$$\tilde{E}_z(a, n, k_z) = \tilde{G}_{zz}^{EJ}(a, n, k_z)\tilde{J}_z(n) \tag{6}$$

where the spectral-domain Green's function $\tilde{G}_{zz}^{EJ}$ is the $\hat{z}$-directed electric field at $\rho = a$ due to a unit-amplitude $\hat{z}$-directed electric current element at (a, ϕ_0, z_0). The full expression is listed in the Appendix.

Then, by applying the boundary condition that the microstripline surface current and the electric field are complementary to each other at $\rho = a$, we can derive

$$\int_{-\phi_a}^{\phi_a} E_z(a, \phi, z)J_z(\phi)a\,d\phi = \sum_{n=-\infty}^{\infty}\tilde{G}_{zz}^{EJ}(a, n, -k_e)J_0^2(n\phi_a)e^{-jk_e z} = 0 \tag{7}$$

where $J_0(n\phi_a)$ is a Bessel function of the first kind with order zero. Thus, by seeking the root of the characteristic equation

$$\sum_{n=-\infty}^{\infty} G_{zz}^{EJ}(a, n, -k_e)J_0^2(n\phi_a) = 0 \tag{8}$$

the effective propagation constant k_e and, in turn, the effective dielectric constant $\epsilon_{eff} = (k_e/k_0)^2$ can be obtained.

As for the calculation of the characteristic impedance of a cylindrical microstripline, we adopt the power-current definition [4], i.e.,

$$Z_c = 2P/I_T^2 \tag{9}$$

where I_T is the total surface current; P is the time-average Poynting power flowing along the z axis inside the region of $0 < \rho < b$ and can be calculated from

$$P = \frac{1}{2}\,\mathrm{Re}\left[\int_0^b\int_0^{2\pi}(\vec{E}\times\vec{H}^*)\cdot\hat{z}\rho\,d\phi\,d\rho\right]. \tag{10}$$

The asterisk denotes a complex conjugate. Then, by applying Parseval's theorem, the time-average power P of (10) can be expressed in the spectral domain as

$$P = \frac{1}{4\pi}\sum_{n=-\infty}^{\infty}(\tilde{P}_1 + \tilde{P}_2) \tag{11}$$

with

$$\begin{aligned}\tilde{P}_1 &= \int_0^a [\tilde{E}_\rho^{(1)}\tilde{H}_\phi^{(1)^*} - \tilde{E}_\phi^{(1)}\tilde{H}_\rho^{(1)^*}]\rho\,d\rho, \\ &= \int_0^a [\tilde{G}_{\rho z}^{EJ^{(1)}}\tilde{G}_{\phi z}^{HJ^{(1)^*}} - \tilde{G}_{\phi z}^{EJ^{(1)}}\tilde{G}_{\rho z}^{HJ^{(1)^*}}]\tilde{J}_z^2(n)\rho\,d\rho,\end{aligned} \tag{12}$$

$$\begin{aligned}\tilde{P}_2 &= \int_a^b [\tilde{E}_\rho^{(2)}\tilde{H}_\phi^{(2)^*} - \tilde{E}_\phi^{(2)}\tilde{H}_\rho^{(2)^*}]\rho\,d\rho, \\ &= \int_0^a [\tilde{G}_{\rho z}^{EJ^{(2)}}\tilde{G}_{\phi z}^{HJ^{(2)^*}} - \tilde{G}_{\phi z}^{EJ^{(2)}}\tilde{G}_{\rho z}^{HJ^{(2)^*}}]\tilde{J}_z^2(n)\rho\,d\rho\end{aligned} \tag{13}$$

where the Green's functions $\tilde{G}_{\rho z}^{EJ^{(i)}}$, $\tilde{G}_{\phi z}^{HJ^{(i)}}$, $\tilde{G}_{\phi z}^{EJ^{(i)}}$, and $\tilde{G}_{\rho z}^{HJ^{(i)}}$, $i = 1, 2$, are given in the Appendix.

III. Numerical Results and Discussion

The effective dielectric constant as a function of $k_0 b$ for various curvilinear coefficients is calculated. The curvilinear coefficient R is defined to be the ratio of inner to outer radii, i.e., R = a/b [2]. A typical result is shown in Fig. 2(a) and (b) for two different stripline widths of $w/h = 1.0$ and 2.0, respectively. The substrate is assumed to have a relative dielectric constant $\epsilon_r = 9.6$. Two data points of a planar microstripline ($R = 1.0$) with $w/h = 1.0$ are also shown in Fig. 2(a) for comparison. It is seen that the obtained effective

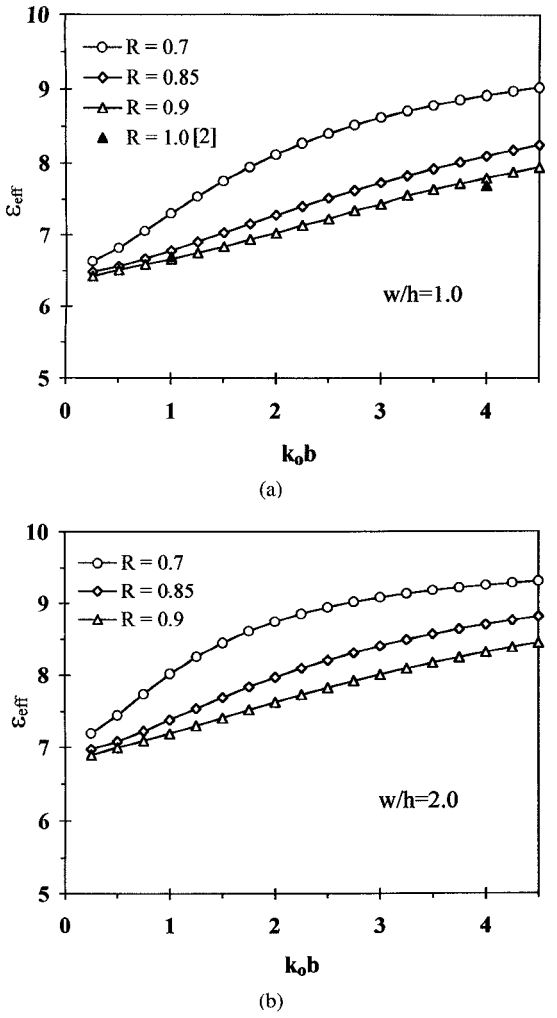

Fig. 2. Effective dielectric constant, ϵ_{eff}, as a function of $k_0 b$ for various curvilinear coefficients; $\epsilon_r = 9.6$, $h = 3.04$ mm. (a) $w/h = 1.0$. (b) $w/h = 2.0$.

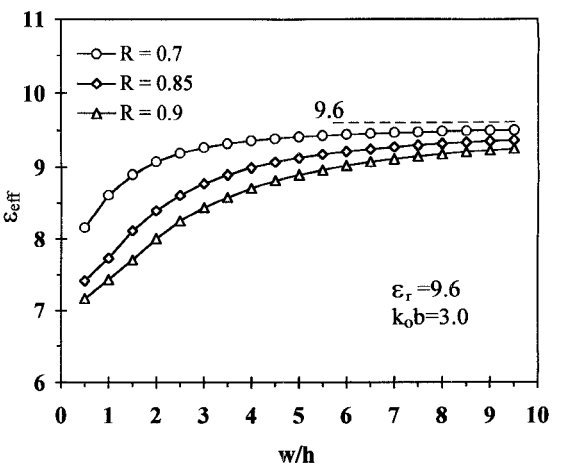

Fig. 3. Effective dielectric constant, ϵ_{eff}, as a function of w/h for various curvilinear coefficients; $\epsilon_r = 9.6$, $h = 3.04$ mm, $k_0 b = 3.0$.

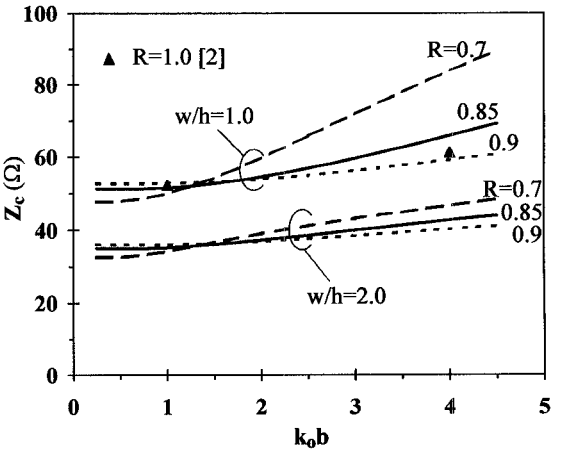

Fig. 4. Characteristic impedance of a cylindrical microstripline as a function of $k_0 b$; $\epsilon_r = 9.6$, $h = 3.04$ mm, $w/h = 1.0$, 2.0.

dielectric constant is very sensitive to the values of R and $k_0 b$. Another interesting result of the dependence of ϵ_{eff} on the stripline width is presented in Fig. 3. It is found that ϵ_{eff} approaches to the value of ϵ_r for a larger stripline width. For the limiting case that the stripline width is 2πa, i.e., the geometry becomes a coaxial line, the value of ϵ_{eff} is found to be the same as ϵ_r.

Fig. 4 shows the results of the characteristic impedance as a function of $k_0 b$. Two stripline widths of $w/h = 1.0$ and 2.0 are presented. It is seen that the obtained characteristic impedance for larger values of R approaches the data points of a corresponding planar microstripline ($w/h = 1.0$). This gives us confidence in the numerical results obtained here. It is also observed that the variation of the characteristic impedance with $k_0 b$ is more sensitive for smaller values of R, and the variation is also more significant for the microstripline with smaller width.

IV. Conclusion

The frequency-dependent characteristics of a cylindrical microstripline mounted inside a ground cylinder are obtained by using an exact Green's-function formulation. Numerical results show that the effective dielectric constant and characteristic impedance of the microstripline are greatly affected by the curvature variation, and strong dispersive behavior of the microstripline is also observed. These are important considerations for the accurate design of such cylindrical microstriplines.

Appendix

There are nine Green's functions derived for this study. They are

$G_{zz}^{EJ} = E_z$ at $\rho =$ a due to a unit-amplitude $\hat{z}$-directed current at (a, ϕ_0, z_0),

$G_{\rho z}^{EJ^{(i)}} = E_\rho$ in region i $(i = 1, 2)$ due to a unit-amplitude $\hat{z}$-directed current at (a, ϕ_0, z_0),

$G_{\phi z}^{HJ^{(i)}} = H_\phi$ in region i $(i = 1, 2)$ due to a unit-amplitude $\hat{z}$-directed current at (a, ϕ_0, z_0),

$G_{\phi z}^{EJ^{(i)}} = E_\phi$ in region i $(i = 1, 2)$ due to a unit-amplitude $\hat{z}$-directed current at (a, ϕ_0, z_0),

$G_{\rho z}^{HJ^{(i)}} = H_\rho$ in region i $(i = 1, 2)$ due to a unit-amplitude $\hat{z}$-directed current at (a, ϕ_0, z_0),

whose spectral amplitudes are, respectively, given as

$$\tilde{G}_{zz}^{EJ}(a, n, k_z) = \frac{j\eta\gamma_1}{D_n k_0}\left(\alpha - \frac{\gamma_1}{\gamma_2}\Delta_2\right),$$

$$\tilde{G}_{\rho z}^{EJ^{(i)}}(\rho, n, k_z) = \frac{\eta\sqrt{\epsilon_{eff}}}{D_n \epsilon_0}\left(\alpha - \frac{\gamma_1}{\gamma_2}\Delta_2\right)M^{(i)} - \sqrt{\epsilon_{eff}}(\epsilon_r - 1)\frac{\eta n^2 k_0^2}{a\rho D_n \gamma_1^2 \gamma_2^2} N^{(i)},$$

$$\tilde{G}_{\phi z}^{HJ^{(i)}}(\rho, n, k_z) = \frac{1}{D_n}\left(\alpha - \frac{\gamma_1}{\gamma_2}\Delta_2\right)M^{(i)} - \epsilon_{eff}(\epsilon_r - 1)\frac{n^2 k_0^2}{a\rho D_n \gamma_1^2 \gamma_2^2} N^{(i)},$$

$$\tilde{G}_{\phi z}^{EJ^{(i)}}(\rho, n, k_z) = j\frac{\eta n\sqrt{\epsilon_{eff}}}{\rho\gamma_1\epsilon_0 D_n}\left(\alpha - \frac{\gamma_1}{\gamma_2}\Delta_2\right)P^{(i)} - j\sqrt{\epsilon_{eff}}(\epsilon_r - 1)\frac{\eta n k_0^2}{aD_n\gamma_1\gamma_2^2} Q^{(i)},$$

$$\tilde{G}_{\rho z}^{HJ^{(i)}}(\rho, n, k_z) = \frac{-n}{\rho\gamma_1 D_n}\left(\alpha - \frac{\gamma_1}{\gamma_2}\Delta_2\right)P^{(i)} + j\frac{n\epsilon_{eff}(\epsilon_r - 1)}{aD_n\gamma_1\gamma_2^2} Q^{(i)}$$

with

$$\eta = \sqrt{\mu_0/\epsilon_0}, \qquad \alpha = \frac{J_n'(\gamma_1 a)}{J_n(\gamma_1 a)},$$

$$X_1 = \frac{H_n^{(1)}(\gamma_2 a)}{J_n(\gamma_2 a)}, \qquad Y_1 = \frac{H_n^{(1)'}(\gamma_2 a)}{J_n'(\gamma_2 a)},$$

$$X_2 = \frac{H_n^{(1)}(\gamma_2 b)}{J_n(\gamma_2 b)}, \qquad Y_2 = \frac{H_n^{(1)'}(\gamma_2 b)}{J_n'(\gamma_2 b)},$$

$$X_3 = \frac{H_n^{(1)}(\gamma_2 \rho)}{J_n(\gamma_2 \rho)}, \qquad Y_3 = \frac{H_n^{(1)'}(\gamma_2 \rho)}{J_n'(\gamma_2 \rho)},$$

$$\gamma_1 = k_0^2 - k_z^2, \qquad \gamma_2 = \epsilon_r k_0^2 - k_z^2,$$

$$M^{(1)} = Q^{(1)} = \frac{J_n'(\gamma_1\rho)}{J_n(\gamma_1 a)}, \qquad N^{(1)} = P^{(1)} = \frac{J_n(\gamma_1\rho)}{J_n(\gamma_1 a)},$$

$$M^{(2)} = \frac{\gamma_1}{\gamma_2}\frac{Y_3 - X_2}{X_1 - X_2}\frac{J_n'(\gamma_2\rho)}{J_n(\gamma_2 a)},$$

$$N^{(2)} = \left(\frac{\gamma_1}{\gamma_2}\right)^2\frac{X_3 - Y_2}{X_1 - Y_2}\frac{J_n(\gamma_2\rho)}{J_n(\gamma_2 a)},$$

$$P^{(2)} = \left(\frac{\gamma_1}{\gamma_2}\right)^2\frac{X_3 - X_2}{X_1 - X_2}\frac{J_n(\gamma_2\rho)}{J_n(\gamma_2 a)},$$

$$Q^{(2)} = \frac{\gamma_1}{\gamma_2}\frac{Y_3 - Y_2}{X_1 - Y_2}\frac{J_n'(\gamma_2\rho)}{J_n(\gamma_2 a)},$$

$$D_n = \epsilon_0\left[\frac{nk_0k_e(\epsilon_r - 1)}{a\gamma_1\gamma_2^2}\right]^2 - \left(\alpha - \frac{\gamma_1}{\gamma_2}\Delta_2\right)\left(\alpha - \frac{\gamma_1}{\gamma_2}\epsilon_r\Delta_1\right),$$

$$\Delta_1 = \frac{H_n^{(1)}(\gamma_2 b)J_n'(\gamma_2 a) - J_n(\gamma_2 b)H_n^{(1)'}(\gamma_2 a)}{H_n^{(1)}(\gamma_2 b)J_n(\gamma_2 a) - J_n(\gamma_2 b)H_n^{(1)}(\gamma_2 a)},$$

$$\Delta_2 = \frac{H_n^{(1)'}(\gamma_2 b)J_n'(\gamma_2 a) - J_n'(\gamma_2 b)H_n^{(1)'}(\gamma_2 a)}{H_n^{(1)'}(\gamma_2 b)J_n(\gamma_2 a) - J_n'(\gamma_2 b)H_n^{(1)}(\gamma_2 a)}.$$

It is also noted that Δ_1 and Δ_2 are calculated using a similar algorithm given in [2], and $J_n(x)$ is a Bessel function of the first kind with order n; $H_n^{(1)}(x)$ is a Hankel function of the first kind with order n. The prime in the equation denotes a derivative with respect to the argument.

References

[1] K. L. Wong and Y. C. Chen, "Resonant frequency of a slot-coupled cylindrical-rectangular microstrip structure," *Microwave Opt. Technol. Lett.*, vol. 7, pp. 566–570, Aug. 20, 1994.

[2] N. G. Alexopoulos and A. Nakatani, "Cylindrical substrate microstrip line characterization," *IEEE Trans. Microwave Theory Tech.*, vol. 35, pp. 843–849, Sept. 1987.

[3] K. L. Wong, Y. T. Cheng, and J. S. Row, "Resonance in a superstrate-loaded cylindrical-rectangular microstrip structure," *IEEE Trans. Microwave Theory Tech.*, vol. 41, pp. 814–819, May 1993.

[4] J. R. Brews, "Characteristic impedance of microstrip lines," *IEEE Trans. Microwave Theory Tech.*, vol. 35, pp. 30–34, Jan. 1987.

Attenuation of the Parasitic Modes in a Shielded Microstrip Line by Coating Resistive Films on the Substrate

Young-Hoang Chou and Shyh-Jong Chung

***Abstract*—In this paper, propagation characteristics of even-symmetric hybrid modes in a waveguide-shielded microstrip line with the presence of the resistive films affixed to the two sides of the center strip is investigated. The method of lines with modifications concerning the inhomogeneity of the surface between the air and substrate layers is used for analysis. After a validity check of the analysis by considering two special structures, i.e., a microstrip line ($R_m = \infty$) and a coplanar waveguide (R_m =0), the resistance R_m and the width W_m of the film are varied to see the influence on the propagation and attenuation constants of the dominant mode as well as the higher-order (parasitic) modes. Optimal combinations of the resistance and the width are found so that the resistive film has the largest attenuating effect on the higher-order modes but has no interference with the dominant one.**

I. Introduction

Microstrip circuits are often enclosed in metal packages to prevent mechanical damage and electromagnetic interferences from the environment and to provide electrical isolation between different parts of the circuits. However, these metal enclosures may have two important influences on the circuit performances. The first is the proximity effect which occurs when the package wall is close to the circuit. The second is the coupling between the circuit signals and the parasitic modes of the housing introduced when the operating frequency is above the cutoff frequency for higher order mode propagation [1], [2]. Proximity effect on the characteristic of the dominant mode can be minimized by the use of an eletrically large enclosure which, however, can support several propagation (parasitic) modes. As indicated in [1], the erratic circuit behaviors caused by the parasitic coupling of these higher-order modes are more important than the proximity effects. Therefore, it is more desirable to device efficient ways to suppress the propagation of these modes.

Several possible approaches for suppressing the parasitic modes were summarized in [3], which included the deformation of the

Manuscript received March 2, 1994; revised Dec. 23, 1994. This work was supported by the National Science Council of the Republic of China Grant NSC 82-0404-E-009-336.

The authors are with the Institute of Communication Engineering, National Chiao Tung University, Hsinchu, Taiwan, R.O.C.

IEEE Log Number 9412061.